Preclinical Development

Molecular Cancer Therapeutics

In Silico Screening Reveals Structurally Diverse, Nanomolar Inhibitors of NQO2 That Are Functionally Active in Cells and Can Modulate NF-κB Signaling

Karen A. Nolan[1], Mark S. Dunstan[2], Mary C. Caraher[1], Katherine A. Scott[1], David Leys[2], and Ian J. Stratford[1]

Abstract

The National Cancer Institute chemical database has been screened using *in silico* docking to identify novel nanomolar inhibitors of NRH:quinone oxidoreductase 2 (NQO2). The inhibitors identified from the screen exhibit a diverse range of scaffolds and the structure of one of the inhibitors, NSC13000 cocrystalized with NQO2, has been solved. This has been used to aid the generation of a structure–activity relationship between the computationally derived binding affinity and experimentally measured enzyme inhibitory potency. Many of the compounds are functionally active as inhibitors of NQO2 in cells at nontoxic concentrations. To show this, advantage was taken of the NQO2-mediated toxicity of the chemotherapeutic drug CB1954. The toxicity of this drug is substantially reduced when the function of NQO2 is inhibited, and many of the compounds achieve this in cells at nanomolar concentrations. The NQO2 inhibitors also attenuated TNFα-mediated, NF-κB–driven transcriptional activity. The link between NQO2 and the regulation of NF-κB was confirmed by using short interfering RNA to NQO2 and by the observation that NRH, the cofactor for NQO2 enzyme activity, could regulate NF-κB activity in an NQO2-dependent manner. NF-κB is a potential therapeutic target and this study reveals an underlying mechanism that may be usable for developing new anticancer drugs. *Mol Cancer Ther; 11(1); 194–203. ©2011 AACR.*

Introduction

Quinone oxidoreductase 2 (NQO2, QR2, EC.1.10.99.2) was first identified by Liao and colleagues (1) as an FAD-containing protein capable of oxidizing a variety of analogues of dihydronicotinamide. It is a homolog of NAD(P)H:quinone oxidoreductase 1 (NQO1, DT-diaphorase, EC.1.6.99.2) with which it shares significant structural similarity. The proteins are homodimeric with 2 active sites comprising residues from both monomers that are located at opposite ends of the dimer. However, major differences exist between the catalytic domains of the 2 enzymes; in particular, the binding pocket of NQO2 is more hydrophobic and slightly larger than NQO1 (2–4). In addition, whereas NQO1 can use NADPH or NADH as reducing cofactors, this does not occur with NQO2 unless the pH is reduced substantially (5). To support the enzymatic activity of NQO2, the most efficient cofactors are *N*-methyl, *N*-benzyl, or *N*-ribosyl nicotinamide (NRH; refs. 6, 7).

The physiologic role of NQO1 is well characterized with its major function being considered to be as a detoxification enzyme (8). A detoxification and/or chemoprotectant role for NQO2 has also been suggested from studies on quinone reduction (9, 10) and the enhanced carcinogen activity of benzo(a)pyrene observed in $NQO2^{-/-}$ mice (11). However, a comparable metabolic role for NQO1 and NQO2 is confounded by the observation that genetic knockout of NQO1 increases menadione toxicity in mice, whereas in NQO2 knockout mice there is protection against menadione toxicity (12,13). Hence, other nonenzymatic properties of the proteins may contribute to the overall physiologic functions of NQO1 and NQO2. This has been the subject of some recent reviews (8, 14, 15). There is growing evidence that both NQO1 and NQO2 can protect against 20S proteasomal degradation of p53 and other onco-proteins (16). In the case of NQO1 the ability to stabilize p53 is NAD(P)H dependent (17). An inference from this is that the protein needs to be in its reduced state to efficiently interact with p53. Inhibitors of NQO1 such as dicoumarol will compete with NAD(P)H for binding to NQO1 and hence prevent reduction of the enzyme bound FAD; thus, dicoumarol promotes degradation of p53 (17, 18). The results of these pharmacologic experiments have been recapitulated in experiments with cells and tissues derived from $NQO1^{-/-}$ mice, which have shown reduced levels of p53 and a variety of other proteins (19). Similar observations were made when investigations were made of p53 levels in cells and tissues from $NQO2^{-/-}$ mice (13).

Authors' Affiliations: [1]School of Pharmacy and Pharmaceutical Sciences, University of Manchester and Manchester Cancer Research Centre; and [2]Manchester Interdisciplinary Biocentre, University of Manchester, Manchester, United Kingdom

Note: Supplementary data for this article are available at Molecular Cancer Therapeutics Online (http://mct.aacrjournals.org/).

Corresponding Author: Ian James Stratford, School of Pharmacy and Pharmaceutical Sciences, University of Manchester and Manchester Cancer Research Centre, Stopford Building, Oxford Road, Manchester M13 9PT, United Kingdom. Phone: 44-0-161-275-2487; Fax: 44-0-161-275-8342; E-mail: ian.stratford@manchester.ac.uk

doi: 10.1158/1535-7163.MCT-11-0543

In addition, genetic knockdown of either NQO1 or NQO2 in mouse keratinocytes revealed that both proteins could play a significant role in NF-κB signaling (20, 21).

The classical inhibitor of NQO2 is resveratrol (4), however, a variety of other structurally diverse inhibitors have been identified (3, 7, 22–25). Many of these inhibitors, including resveratrol, imatinib, and melatonin (26, 27), have other substantive pharmacologic properties, which make them less than ideal for probing the cellular function of NQO2. Thus, we recently embarked on a virtual screening strategy to identify potential candidate ligands for NQO2 (3, 22, 23). To achieve this, we took the crystal structure of NQO2 (PDB code 1QR2, resolution at 2Å; ref. 2) and used a hierarchical *in silico* screening approach to mine the entire National Cancer Institute (NCI) database using computational molecular docking. A range of the 250 top-ranked ligands, including various quinolines, elipticines, acridines, and furanylamidines were made available by the NCI and assessed for their effects on the enzymatic activity of NQO2. Here, we report many of these compounds to be active at nanomolar concentrations as enzyme inhibitors. In addition, we have solved the crystal structure of NQO2 containing one of the inhibitors, NSC13000 (9-aminoacridine) and used this to generate a structure–activity relationship. Compounds, representative of the different structural classes, are also shown to be functionally active as inhibitors of NQO2 enzymatic activity in cells at nontoxic concentrations. This is shown by taking advantage of the selective ability of human NQO2 to activate the drug CB1954 (5-(-aziridin-1-yl)-2,4-dinitrobenzamide) to give a potent cytotoxin (6). Thus, inhibition of the cellular toxicity of CB1954 in air can be regarded as a surrogate measure of the inhibitory potency of the different compounds in cells.

It is known that NF-κB–mediated transcription is a common feature of many tumor types (28) and blockade of NF-κB can cause cell death and tumor regression (28, 29). The cellular activity of NQO2 has been linked to NF-κB signaling (20, 21, 30). Here, we show for the first time that the cofactor for NQO2 activity, NRH, can stimulate the function of NF-κB and that this occurs in a NQO2-dependent manner. Furthermore, it is shown that the potent, structurally diverse inhibitors of NQO2 can also modulate NF-κB signaling. Many of these inhibitors have already been shown to possess anticancer activity and it is likely that this effect on NQO2/NF-κB may contribute to the overall efficacy of these agents. However, now that we have a more precise mechanistic understanding of this process, it provides a rationale for developing NQO2 inhibitors as therapeutic agents in the treatment of cancer.

Materials and Methods

Reagents, chemicals, and NQO2 inhibitors

Unless otherwise stated, all reagents and chemicals were obtained from Sigma-Aldrich. NQO2 inhibitors were made available by the NCI. The structures of all the compounds are given in the Supplementary Table S1. Any compounds that were recognized as being commercially available were obtained from Sigma-Aldrich.

Computational analysis

For molecular docking, the crystallographic coordinates of the human NQO2 (PDB code 1QR2, resolution at 2Å; ref. 2) were obtained from the Brookhaven Database. Hydrogen atoms were added to the structure allowing for appropriate ionization at physiologic pH. The FAD fragment was reatom typed to avoid underestimation by ChemScore of lipophilic–aromatic interactions (31). The protonated complex was minimized within SYBYL 7.3 while holding all heavy atoms stationary. The NCI database was docked as described previously (3), and a range of the 250 top-ranked ligands were made available by the NCI and used for biochemical evaluation.

Protein expression, purification, and crystallography

The overexpression of NQO2 was done in BL21 Codon+ cells. Cells were grown to late log phase before being induced with 1 mmol/L IPTG overnight at 20°C. NQO2 was purified to homogeneity by HisTrap HP Ni^{2+}-affinity chromatography followed by size exclusion chromatography on a Superdex S200 10/300 GL column. Samples were concentrated to approximately 15 mg/mL and supplemented with 5 μmol/L FAD.

The NQO2–NSC13000 complex was obtained by cocrystallization with a 3:1 molar access of NSC13000 (PDB code–3TZB). Conditions were identified using the clear strategy II matrix screen (Molecular Dimensions) on a Mosquito nanodrop crystallization robot. Crystals suitable for diffraction experiments were obtained by sitting drop vapor diffusion in 400 nL drops containing equal volumes of protein and a solution containing 0.15 mol/L potassium thiocyanate, 0.1 mol/L sodium cacodylate pH 6.5, and 20% PEG 1.5K. Data were collected on beamline I04 at the Diamond Light Source Facility and reduced and scaled with the X-ray Detector Software suite (32).

The crystal structure of NQO2–NSC1300 was determined by molecular replacement using PHASER from PHENIX (33) and the NQO2 structure, 1QR2 (2) as a start model. The models were completed by iterative cycles of manual model building and real space refinement using the Coot program (34) and crystallographic refinement using phenix.refine (33). Structure validation was done with Molprobity. The processing and final refinement statistics are given in Supplementary Table S2.

Enzyme assays, cellular enzyme activity, cell lines, and culture

Recombinant human NQO1 and NQO2 were taken and diluted in 50 mmol/L phosphate buffer to give an enzyme activity that would result in a change in optical absorbance of substrate of approximately 0.1 per minute. Inhibition of NQO1 and NQO2 activity was carried out as described previously (22) using 200 μmol/L NADH or NRH (synthesized in-house by converting NADH to NRH

via the use of phosphodiesterase and alkaline phosphatase) as reducing cofactors, and dichlorophenolindophenol (DCPIP) as the substrate. Assays were carried out in the presence or absence of 2 μmol/L bovine serum albumin (BSA). IC_{50} values were determined using nonlinear curve fitting as implemented in the program Excel (GraphPad) for which a 50% reduction of the initial rate was attained. Each measurement was made in triplicate and the experiments were carried out 3 times. IC_{50} values, given in Table 1, are derived from each of these determinations.

For enzyme activity in cells, exponentially growing cultures were washed with PBS, scraped into 50 mmol/L phosphate buffer (pH 7.4) containing 5 μmol/L FAD and 250 mmol/L sucrose, sonicated twice for 5 seconds while on ice, and centrifuged at 13,000 rpm for 15 minutes at 4°C. Protein concentrations were determined using the bicinchoninic acid protein assay and enzyme activities

Table 1. Compounds obtained from the NCI, their broad structural class (individual structures provided in Supplementary Material), ability to inhibit the enzymatic activity of recombinant NQO2 in the presence and absence of BSA, their experimentally determined binding affinity, computationally derived binding affinity, and toxicity toward K562 and MDA-MB-468 cells

NSC number	Structural class[a]	IC_{50}–BSA (μmol/L)	IC_{50} + BSA (μmol/L)	ΔG_{exp} (kJ/mol)	ΔG_{calc} (kJ/mol)	96-h toxicity in cells IC_{50} (μmol/L)	
						K562	MDA-MB-468
9858	A	0.35 ± 0.11	2.46 ± 0.82	−37.08	−56.71	8.7 ± 2.4	3.1 ± 1.0
11232	A	0.60 ± 0.10	5.40 ± 0.90	−35.74	−53.14	69 ± 41	21 ± 13
12547	B	0.16 ± 0.05	1.70 ± 0.80	−39.04	−58.83	5.9 ± 4.2	7.9 ± 2.9
13000	C	0.42 ± 0.15	0.76 ± 0.25	−36.63	−53.73	1.0 ± 1.4	1.1 ± 0.35
13484	D	0.55 ± 0.05	0.86 ± 0.15	−35.96	−57.21	0.44 ± 0.57	0.92 ± 0.064
14229	C	0.2 ± 0.05	8.50 ± 1.60	−38.48	−54.95	4.0 ± 3.6	1.7 ± 0.60
17602	E	0.14 ± 0.04	0.17 ± 0.05	−39.37	−54.94	2.3 ± 2.0	0.66 ± 0.56
28487	A	0.15 ± 0.05	2.40 ± 0.56	−39.20	−55.85	77 ± 16	4.9 ± 3.5
64924	A	0.22 ± 0.06	5.20 ± 1.32	−38.24	−57.23	>100	34 ± 0.19
71795	B	0.05 ± 0.01	0.24 ± 0.09	−42.15	−59.29	0.73 ± 0.60	0.27 ± 0.20
76750	D	0.50 ± 0.06	2.70 ± 0.59	−36.19	−54.26	11 ± 3.8	11 ± 2.5
101984	D	0.64 ± 0.05	2.30 ± 0.70	−35.58	−55.39	>100	3.5 ± 0.32
140268	A	0.06 ± 0.01	6.80 ± 1.71	−41.48	−60.91	28 ± 2.9	29 ± 0.49
156529	A	0.03 ± 0.01	0.80 ± 0.10	−43.67	−62.63	0.12 ± 0.042	0.71 ± 0.22
164016	B	0.02 ± 0.01	3.00 ± 1.21	−44.94	−64.06	0.70 ± 0.29	0.43 ± 0.24
164017	B	0.04 ± 0.01	0.30 ± 0.12	−42.56	−62.87	0.68 ± 0.39	0.72 ± 0.38
219733	C	0.18 ± 0.03	5.40 ± 1.15	−38.74	−61.34	0.022 ± 0.011	0.096 ± 0.085
270904	D	0.17 ± 0.09	5.70 ± 1.31	−38.89	−58.44	3.1 ± 3.6	5.1 ± 3.6
273829	D	0.25 ± 0.05	7.20 ± 1.08	−37.92	−56.25	13 ± 22	16 ± 7.4
305831	E	0.63 ± 0.07	2.80 ± 0.61	−35.62	−57.01	27 ± 35	11 ± 2.6
305836	E	0.05 ± 0.01	0.20 ± 0.09	−42.15	−59.66	5.5 ± 3.6	3.9 ± 2.5
322087	B	0.03 ± 0.00	0.34 ± 0.05	−43.13	−61.73	14 ± 6.3	18 ± 16
356821	A	0.24 ± 0.02	2.80 ± 0.98	−38.03	−58.91	>100	20 ± 1.8
374718	A	0.05 ± 0.01	1.60 ± 0.49	−42.20	−57.92	>100	18 ± 1.6
407356	A	0.80 ± 0.08	10.70 ± 5.00	−35.02	−58.26	11 ± 7.1	0.12 ± 0.11
617933	D	0.04 ± 0.01	0.04 ± 0.004	−42.49	−59.38	1.8 ± 1.6	2.8 ± 1.1
617939	D	0.07 ± 0.01	0.08 ± 0.008	−41.28	−58.65	1.8 ± 1.2	1.1 ± 0.72
620318	A	0.20 ± 0.01	4.10 ± 1.05	−38.48	−57.45	35 ± 33	22 ± 9.1
628440	A	0.66 ± 0.08	9.80 ± 0.92	−35.50	−57.42	0.75 ± 0.76	4.0 ± 0.021
633239	A	0.12 ± 0.03	17.70 ± 5.29	−39.75	−56.56	>100	157 ± 10
648424	A	0.14 ± 0.03	2.60 ± 0.95	−39.37	−55.88	7.4 ± 10	21 ± 0.53
658835	A	0.76 ± 0.12	0.18 ± 0.05	−35.15	−57.44	0.18 ± 0.15	0.30 ± 0.18
682454	A	0.08 ± 0.02	1.50 ± 0.10	−40.77	−59.11	7.9 ± 11	0.11 ± 0.033
Resveratrol	_	0.45 ± 0.15	8.80 ± 1.95	_	_	72 ± 5.1	59 ± 7.2
Imatinib	_	0.03 ± 0.007	0.029 ± 0.01	_	_	0.68 ± 0.51	2.3 ± 0.351

[a]A, poly (fused) aromatic; B, ellipticine; C, acridine; D, quinoline; E, furanylamidine.

determined by adding 10 μL of cell lysate to the reaction mixtures detailed above. The difference in the rates of reaction in the presence and absence of either dicoumarol (100 μmol/L) or resveratrol (1 mmol/L) was used to define NQO1 and NQO2 activity in the cellular lysates respectively.

MDA-MB-468 and BT474 breast cancer cells and K562 chronic myelogenous leukemia cells were obtained from the American Type Culture Collection. MDA-MB-468 and K562 cells were chosen because they express relatively high levels of NQO2 (219 ± 89 and 319 ± 92 nmoles DCPIP reduced/min/mg protein, respectively), with the activity of NQO1 being comparatively lower (8.5 ± 3.1 and 30.6 ± 13.7 nmoles DCPIP reduced/min/mg protein, respectively). BT474 cells express substantially less NQO2 compared with the other cells lines (4.2 ± 2.0 nmoles DCPIP reduced/min/mg protein). Cells were maintained in exponential phase in RPMI-1640 medium (Invitrogen) supplemented with 10% (v/v) heat-inactivated fetal calf serum (FCS; Biosera) and 2 mmol/L L-glutamine (Invitrogen).

Macrophage culture and measurement of nitrite

The mouse macrophage cell line J774.2 was grown in Dulbecco's Modified Eagle's Medium supplemented with 10% FCS and 2 mmol/L L-glutamine. Macrophages (3×10^6) were plated in 6-cm plates in serum-free medium for 24 hours before they were exposed to a combination of 25 ng/mL IFN-γ and 100 μg/mL LPS with or without the putative NQO2 inhibitors for 24 hours. Following treatment, the cytokines were washed out and serum was returned into the medium. The cells were reincubated for another 24 hours, at which point the culture medium was collected for subsequent measurement of nitrite levels using the Griess reaction. The amount of nitrite accumulated in the medium of cells can be used as a surrogate measure of NO production, which occurs as a consequence of induction of iNOS by the cytokine treatment (35).

NQO2 short interfering RNA transfection

MDA-MB-468 cells were seeded (7×10^5) into 6-cm plates and allowed to adhere for 24 hours. Human NQO2 short interfering RNA (siRNA; GAAUGUGGCUGUAGAUGAAUU; Thermo Scientific Dharmacon) was transiently transfected (100 nmol/L) using oligofectamine transfection reagent diluted in opti-MEM media. After 5 hours of incubation at 37°C, 5% CO_2 the medium was replaced with RPMI supplemented with 10% FCS. Maximum reduction of NQO2 was seen at 48 hours posttransfection.

Assays of toxicity

MDA-MB-468 cells were seeded at 2.5×10^3 cells per well in 96-well plates and exposed to compounds in full growth media for 3, 24, or 96 hours. For the shorter exposure times, drug was removed and replaced with fresh media and allowed to grow on for a total of 96 hours. The number of surviving cells was then determined using the MTT assay (22). All toxicity experiments were repeated on at least 3 separate occasions. Data were analyzed and curves drawn using the GraphPad Prism5 software package. K562 cells were seeded at 5×10^3 cells per well in 96-well plates and exposed to increasing concentrations of the NCI compounds for 96 hours. The number of surviving cells was then determined using the XTT colorimetric dye reduction assay (36).

To determine the potency at which the compounds could inhibit the cellular activity of NQO2, cells were treated for varying times (3, 24, or 96 hours), with either a fixed concentration of inhibitor and varying concentrations of CB1954 or a fixed concentration of CB1954 and varying concentrations of the putative inhibitors. As above, for the shorter time points, the cells were then washed with PBS and fresh media added. The plates were incubated for a total of 96 hours and the MTT (or XTT) assay was used to determine cell viability.

Plasmids

Two luciferase plasmids were purchased from SA Biosciences. The Cignal NF-κB reporter plasmid contains an inducible firefly luciferase construct and constitutively expressing *Renilla* luciferase construct. The Cignal Positive Control plasmid contains constitutively expressing firefly luciferase and *Renilla* luciferase constructs. The inducible firefly reporter construct is controlled by a basal promoter element (TATA box), which is driven by a 6 times transcriptional response element specific for NF-κB. The constitutive *Renilla* reporter construct is under the control of the *CMV* promoter (37).

Luciferase reporter assay

MDA-MB-468 cells were seeded (7×10^5) into 6-cm plates and allowed to adhere for 24 hours. Expression plasmids were transiently transfected (1 μg/plate) using oligofectamine transfection reagent (Invitrogen) diluted in opti-MEM (Invitrogen Gibco) according to manufacturer's instructions. After 5 hours of incubation at 37°C, the medium was replaced with RPMI plus 10% FCS and cells reseeded into a 96-well plate. The cells were treated for 1 hour with 100 μmol/L NRH and/or 20 ng/mL TNFα (Invitrogen), then given various concentrations of inhibitor [dissolved in dimethyl sulfoxide (DMSO) to a final concentration of no more than 0.5%] for 18 hours. Cells were then lysed with passive lysis buffer, 20 μL of lysate was transferred into a white-walled 96-well plate and assayed using the Dual-Luciferase Reporter Assay System (Promega) on a BMG Labtech Microplate Luminometer.

Results

Structure–activity relationships

The computationally derived calculated and experimentally determined binding affinities of the top ranked compounds supplied by the NCI are given in Table 1. Also included in the table are values of IC_{50} for their inhibition of NQO2 in the presence and absence of

BSA, together with the IC_{50} for the toxicity of the compounds toward MDA-MB-468 cells and K562 cells. The inhibitors listed in Table 1 have also been given a designation indicating their structural class [A–poly (fused) aromatic, B–ellipticine, C–acridine, D–quinoline, and E–furanylamidine]. Figure 1 gives an example of the binding mode of a compound from classes A, B, D, and E. The binding of NSC620318, a poly (fused) aromatic compound, is shown in panel A. The compound has a binding energy of −57.45 kcal/mol, an IC_{50} of 200 nmol/L, and forms π-π stacking interactions with the isoalloxazine ring of FAD, and hydrophobic contacts with W105′, F126, F131, and F178. It also forms hydrogen bond interactions with Y155′ (2.8 Å), N161′ (2.8 Å), and G174 (2.7Å). Panel B shows the binding of the elipticine analog NSC164016. This compound is the highest scoring ligand with a binding energy of −64.06 kcal/mol and an IC_{50} of 20 nmol/L. It forms π-π stacking interactions with FAD and hydrophobic contacts with W105′, Y132, F126, F131, and F178. Panel C shows the quinoline, NSC617933 binding in the active site of NQO2. This compound has a binding energy of −59.38 kcal/mol and an IC_{50} of 40 nmol/L. It forms hydrophobic contacts with active site residues W105′, F126, and F178, π-π stacking interactions with FAD, and has hydrogen bond contacts with T71 (2.4 Å), the carbonyl backbone of D117 (3.0 Å) and Q122 (2.8 Å and 3.1 Å). The related compound, NSC14229 (quinacrine) is the only compound from this panel that has previously been reported as an inhibitor of NQO2 (7). The binding mode of the furanylamidine, NSC305831 is given in panel D. This compound has a binding energy of −57.01 kcal/mol and an IC_{50} of 630 nmol/L. It forms hydrophobic interactions with W105′, F126, and F178 and hydrogen bond contacts with D117 (2.1 Å), R118 (2.8 Å), Y132 (3.0 Å), G174 (2.9 Å), and N161′ (3.1 Å). Interestingly, the related compound NSC305836 is a more potent inhibitor with an IC_{50} of 50 nmol/L. This ligand has 2 additional methyl groups on the furanyl ring that results in additional binding with W105′ and F106′.

NSC13000 has a binding energy of −53.73 kcal/mol and an IC_{50} of 420 nmol/L. The X-ray crystal structure of the ligand bound in the active site of NQO2 is shown in Supplementary Fig. S1. NSC13000 interacts primarily via stacking interactions with the conjugate ring system of FAD and the side chain of F178. The isoalloxazine ring of FAD provides the floor of the active site and stacks with the acridine moiety of NSC13000. Hydrophobic residues F126 and F178 form the ceiling of the binding site, whereas W105′ (primes denote residues from the other NQ02 protomer) sits at the back of the binding pocket and forms a hydrophobic interaction with the amine face of NSC13000. For comparative purposes, the docking orientation of the compound superimposed on to the crystal ligand is given in the Supplementary Fig. S2 and shows excellent concordance between the docking modes with a root mean square distance of 1.26 Å.

A plot of the calculated binding energies for all the compounds versus the experimentally measured binding energy [derived from the Cheng–Prusoff equation (ref. 38), which uses the IC_{50} values for enzyme inhibition] is shown in Supplementary Fig. S3 and from this analysis, a correlation coefficient of $R^2 = 0.52$ was determined.

All of the compounds were also tested for their ability to inhibit NQO1. No inhibition was observed for any of the compounds (up to 100 μmol/L), with the exception of NSC628440, which we had previously reported (39) to be a relatively weak inhibitor. Compounds were also evaluated for their toxicity toward MDA-MB-468 and K562 cells, both of which express relatively high levels of NQO2 (Table 1). Values of IC_{50} for toxicity vary over 1,000-fold

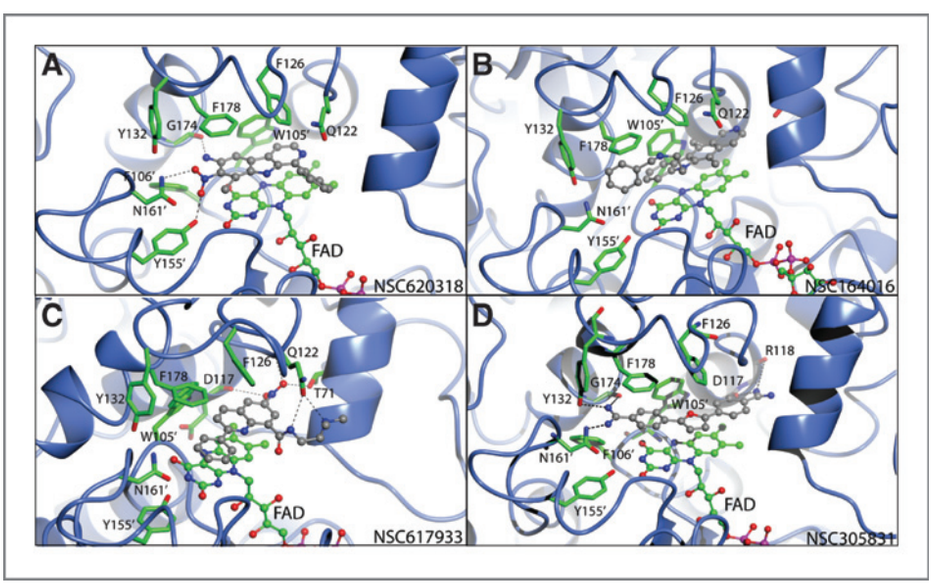

Figure 1. Detailed view of NSC620318 (A), NSC164016 (B), NSC617933 (C), and NSC305831 (D) bound in the NQO2 active site. The individual monomers are colored in blue, key active site residues and the FAD cofactor are shown in green, with hydrogen bonds indicated by black dotted lines.

in both cell lines, and there is no clear relationship between NQO2 inhibitory potency and toxicity.

Functional activity as inhibitors of NQO2 in cells

In our previous work on NQO1, we took advantage of its ability to activate the anticancer drug EO9 [5-aziridinyl-3-hydroxymethyl-2-(3-hydroxyprop-1-enyl)-1-methylindole-4,7-dione, Apaziquone] to show the functional activity of the enzyme in cells. This then allowed assessment of the ability of various coumarin-based compounds to act as inhibitors in cancer cells (40, 41). A similar approach was taken here to determine the ability of the compounds identified as potent inhibitors of NQO2 to be functionally active in cells. To do this, we used the unique ability of NQO2 to activate CB1954 to give a potent cytotoxin (6). To validate the approach, MDA-MB-468 cells were used as they possess relatively high levels of NQO2. Cells were first treated with varying concentrations of CB1954 for 3 hours at 37°C. The closed circles in Fig. 2A show that concentrations of CB1954 in excess of 1 mmol/L are needed to achieve a value for IC_{50}. Previously, it was shown that the enzymatic activity of NQO2 is supported by the cosubstrate, NRH, which exists at only very low concentrations in cells (6). Therefore, varying concentrations of NRH (1 μmol/L to 1 mmol/L) were added to cells together with the CB1954. Results are given in Fig. 2A and show that the added NRH causes a substantial increase in the toxicity of CB1954. NRH itself at these concentrations shows no toxicity. As has previously been suggested (6), this strongly suggests that it is the NQO2-supported reductive activation of CB1954 that leads to toxicity. To support this contention, similar experiments were carried out with BT474 cells that express very low levels of NQO2. Data are given in Supplementary Fig. S4 and show that in the absence of NRH, the IC_{50} value for CB1954 is in excess of 1 mmol/L, whereas in the presence of 100 μmol/L NRH there is a small increase in cellular sensitivity to give an IC_{50} of 1 mmol/L. Finally, to confirm these observations, MDA-MB-468 cells were transfected with siRNA to NQO2. Western blotting indicated that after 48 hours, NQO2 levels reached a nadir (Fig. 2D), and this was consistent with a measured 60% reduction in enzyme activity (to 93 ± 40 nmol DCPIP reduced/min/mg of protein) at that time. Cells were then treated with varying concentrations of CB1954 plus 100 μmol/L NRH. Results shown in Fig. 2B clearly indicate that downregulation of NQO2 causes a decrease in the toxicity of CB1954.

These results provided a platform for evaluating the ability of the compounds described above to be functionally active as inhibitors of NQO2 in cells. To do this, MDA-MB-468 cells were treated with 100 μmol/L CB1954, in the presence of 100 μmol/L NRH, together with varying concentrations of the putative inhibitors for 3 hours. The maximal concentration of each compound tested depended on solubility and/or final concentration of vehicle (DMSO) or the toxicity of the inhibitor. An amount of 100 μmol/L CB1954 plus 100 μmol/L NRH reduces proliferation of MDA-MB-468 cells to about 25%; therefore, adding increasing concentrations of enzyme inhibitor should elicit a steady decrease in toxicity of CB1954. Fig. 2C shows representative dose–response curves for MBA-468 cells exposed to 100 μmol/L CB1954 and some of the NQO2 inhibitors, and it is clear that protection efficiency varies between the different compounds. Similarly, experiments were carried out with

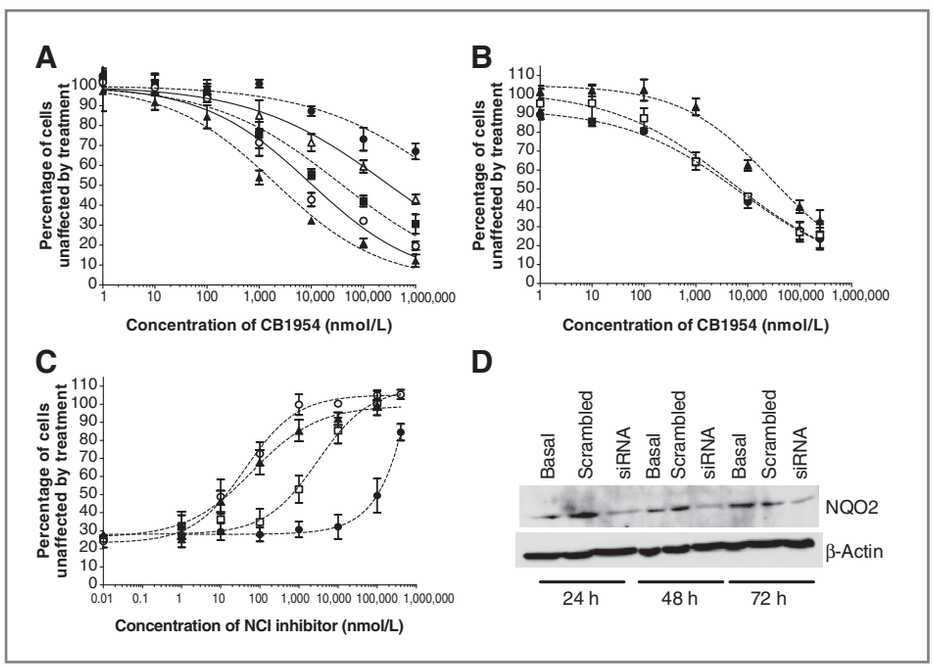

Figure 2. Sensitivity of MDA-468 cells exposed to CB1954 for 3 hours. A, cells treated in the presence or absence of NRH (●, CB1954 alone; △, CB1954 + 1 μmol/L NRH; ■, CB1954 + 10 μmol/L NRH; O, CB1954 + 100 μmol/L NRH; ▲, CB1954 + 1,000 μmol/L NRH). B, MDA-468 cells transfected with siRNA to NQO2, then 48 hours later treated with varying concentrations of CB1954, together with 100 μmol/L NRH (●, control; □, scrambled oligo; ▲, siNQO2). C, protection against the toxicity of 100 μmol/L CB1954 (in the presence of 100 μmol/L NRH) by varying concentrations of some of the NQO2 inhibitors. O, NSC71795; ▲, NSC13000; □, NSC620318; ●, Resveratrol. D, Western blots showing reduction in the level of NQO2 following treatment of MDA-MB-468 cells with siRNA.

different concentrations of inhibitors with varying concentrations of CB1954. Examples are given in Supplementary Fig. S5 and show that low nanomolar concentrations of the inhibitors can alter the toxicity of CB1954. To compare the inhibitory potency of the structurally diverse compounds, the concentration needed to inhibit the toxicity of 100 μmol/L CB1954 by 50% was determined. These values of IC_{50} for protection against CB1954 toxicity are given in Table 2 and they differ by more than 1,000-fold. NSC71795 seems to be the most potent compound for protecting against the toxicity of CB1954 in MDA-MB-468 cells, and the concentration required to reduce toxicity by 50% is 0.054 μmol/L. In contrast, resveratrol, the classical inhibitor of NQO2 is substantially less efficient with an IC_{50} value of approximately 150 μmol/L. Also shown in Table 2 are the values for the toxicity of the putative inhibitors when given to MDA-MB-468 cells alone for 3 hours. In most instances, the ability of the compounds to inhibit the toxicity of CB1954 (i.e., inhibit the activity of NQO2) occurs at significantly lower concentrations than those that, by themselves, are toxic.

Effect of NQO2 inhibitors on the activity of NF-κB

Our discovery of potent inhibitors of NQO2 came from computational screening of the NCI database. The compounds that emerged from this study represented a wide variety of structural classes including elipticines, acridines, quinolines, and furanyl amidines. Interestingly, when carrying out a Prediction of Activity Spectra for Substances (PASS) analysis of these compounds using the NCI database (42), some of the agents showed high PASS-predicted probabilities for them to have anti-inflammatory properties and/or inhibitory effects on release of TNFα. Such an analysis can only provide a pointer to activity, however, it is known that some compounds that can inhibit the activity of recombinant NQO2 can also impair gene transcription regulated by TNFα (25, 30). We, therefore, carried out experiments to determine whether compounds representative of the diverse structural classes identified above that are functionally active as inhibitors of NQO2 in cells could alter TNFα-driven NF-κB–mediated gene transcription. In addition, we evaluated whether any drug induced effects on NF-κB processes were NQO2 dependent.

Table 2. Exposure of MDA-MB-468 cells to a variety of the NQO2 inhibitors for 3 hours in the presence or absence of 100 μmol/L CB1954 plus 100 μmol/L NRH

NCI compound	3-h toxicity (IC_{50}) inhibitor alone (μmol/L)	3-h IC_{50} (μmol/L) inhibitor + CB1954/NRH
Resveratrol	>100	146 ± 103
12547	42 ± 16	0.99 ± 0.23
13000	23 ± 5.1	0.26 ± 0.18
17602	8.9 ± 4.0	0.67 ± 0.15
71795	1.9 ± 0.76	0.054 ± 0.053
164016	1.4 ± 0.29	2.3 ± 1.9
164017	1.8 ± 0.10	0.56 ± 0.26
219733	0.25 ± 0.074	0.33 ± 0.19
305831	114 ± 52	4.3 ± 3.8
305836	14 ± 2.0	18 ± 16
322087	49 ± 25	15 ± 13
617933	12 ± 2.2	0.51 ± 0.43
617939	5.1 ± 2.3	0.38 ± 0.27
620318	>100	2.1 ± 1.2

NOTE: The value of IC_{50} given for cells exposed to inhibitor plus CB1954/NRH is the concentration of inhibitor required to reduce the toxicity of CB1954/NRH by 50%.

Experiments were carried out in MDA-MB-468 cells transiently transfected with a dual-luciferase construct containing a CMV-driven *Renilla* reporter and an NF-κB responsive firefly reporter. First, we evaluated the effect of treating cells with TNFα for 18 hours on luciferase activity. Untreated, exponentially growing MDA-MB-468 cells show a small but significant level of NF-κB–mediated transcription, which was increased almost 3-fold by treatment with 20 ng/mL TNFα (Fig. 3A). Because NRH can modulate the functionality of NQO2 in cells, we also carried out experiments in which 100 μmol/L NRH was added to cells with and without TNFα. These results are also given in Fig. 3A and showed that addition of the cofactor NRH stimulates NF-κB activity to a similar level to that seen with TNFα, but combining NRH with TNFα gives no additional effect. This interesting observation may point to a redox-based mechanism linking NQO2 activity and NF-κB function and this is the subject of further investigation. To confirm that the effects were dependent on NQO2, MDA-MB-468 cells were transfected with siRNA to NQO2 and, 48 hours later, treated with or without TNFα. These results are given in Fig. 3B and showed that the reduction in NQO2 activity brought about by the transfection of siRNA causes a reduction in the basal expression of NQO2. Furthermore, the induction of NF-κB by TNFα is also significantly decreased by the reduction in NQO2 activity. The NQO2 inhibitor, NSC13000, was then evaluated for its ability to modulate NF-κB transcriptional activity in MDA-468 cells treated with or without NRH. Results are given in Fig. 3C for cells treated with 0.1 μmol/L NSC13000, and it is clear that drug treatment reduces the luciferase activity in both treatment groups. We then went on to determine whether a range of NQO2 inhibitors, representative of the different structural classes (structures given in Fig. 4B), could attenuate the increase in NF-κB activity caused by treatment with NRH and TNFα. Results given in Fig. 4A show that each of the compounds, at 0.1 μmol/L, can cause a substantial reduction in NF-κB activity. These results were confirmed by the indirect measurement of the activity of an NF-κB target gene (iNOS) in cytokine stimulated mouse macrophages treated with the different inhibitors. The concentration of nitrite in growth medium is a

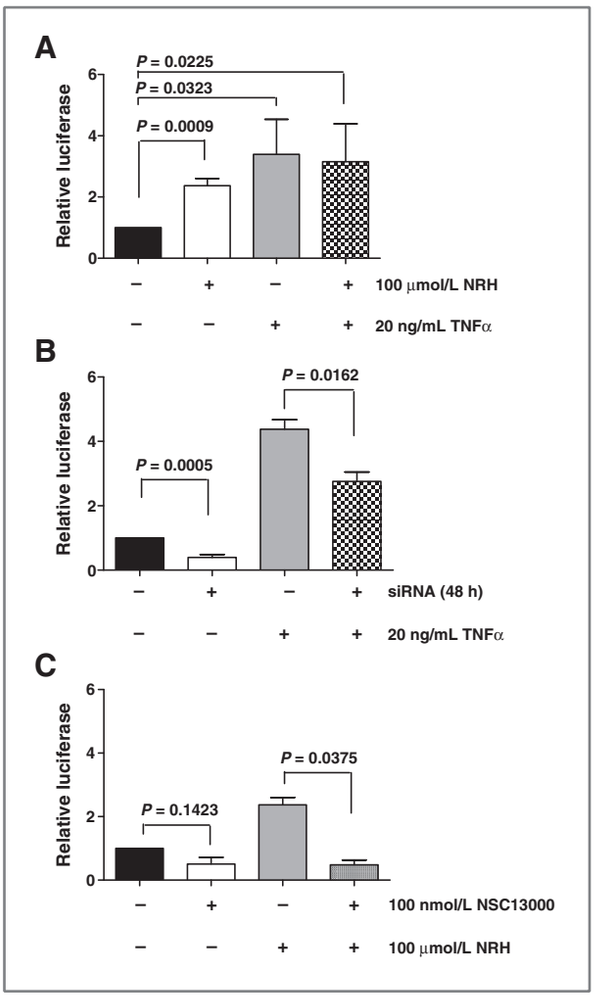

Figure 3. Luciferase levels in MDA-MB-468 cells exposed to 20 ng/mL TNFα and/or 100 μmol/L NRH. A, effect of NRH and TNFα used alone or in combination. B, cells with NQO2 levels reduced by before treatment with siRNA, then induced with TNFα. C, cells treated with 100 nmol/L NSC13000 and/or NRH.

measure of the activity of iNOS and Fig. 4A also shows that each of the compounds given to macrophages at a concentration of 0.125 μmol/L for 24 hours results in a reduction in the level of nitrite. Examples of 6 further compounds attenuating NF-κB activity and nitrite production are given a supplementary Fig. S6.

Discussion

In this work, virtual screening of the NCI database has revealed novel, nanomolar inhibitors of NQO2 and shown that these compounds are functionally active as enzyme inhibitors in cells. Using an NF-κB reporter assay, it is shown that the cofactor for NQO2 enzymatic activity, NRH, can induce *NF-κB* gene transcription, and this induction is similar to that level of induction seen with TNFα. The induction of NF-κB activity is reduced by the NQO2 inhibitors, and this observation is recapitulated when enzyme activity is reduced by transfection of siRNA to NQO2. Hence, we have provided some evidence to suggest a causal link between the activity of NQO2 and the regulation of NF-κB and that this can be modulated by a variety of structurally diverse inhibitors of NQO2.

There has been a recent plethora of publications on the synthesis of potential inhibitors of NQO2 (3, 7, 22–26, 43, 44). The work of the Boutin group (7, 26) has focused on the observation that NQO2 is the third melatonin binding site, MT3. From these studies, the fused poly heteroaromatic compound S29434 was identified as a nanomolar inhibitor of recombinant NQO2 with the ability to compete with melatonin for binding. In contrast, the Cushman group (24, 25) have concentrated on the potential cancer chemoprotective activity of resveratrol analogues and substituted phenazines. They measured inhibition of recombinant NQO2 (with several compounds active in the nanomolar range), as well as measuring effects on

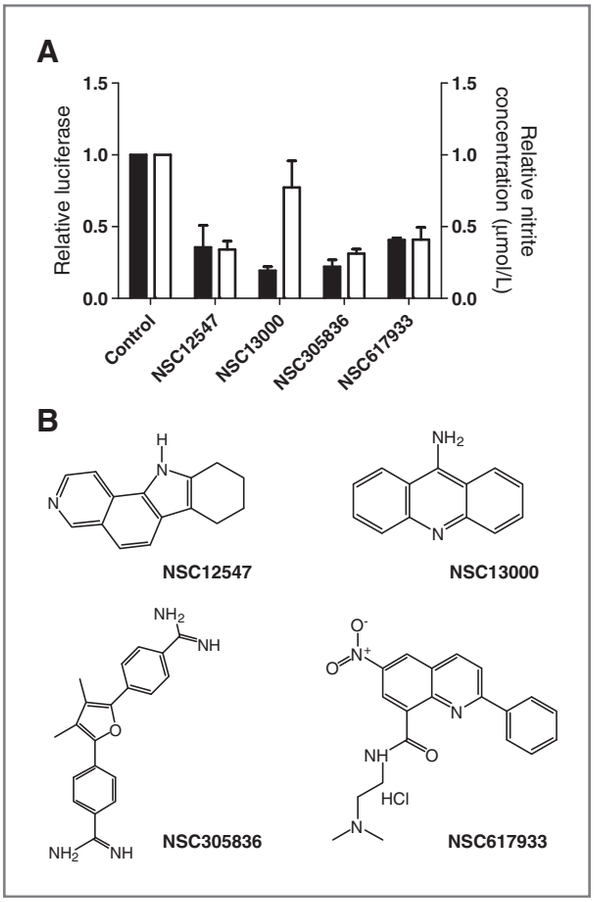

Figure 4. A, solid bars, NF-κB activity in MDA-MB-468 cells treated with 100 μmol/L NRH and 20 mg/mL TNFα plus a variety of the NSC compounds at a concentration of 100 nmol/L; open bars, effects of the NQO2 inhibitors (125 nmol/L) on nitrite production by J774.2 cells treated with LPS and IFNχ. B, structures of the compounds used to generate the data in A.

iNOS activity and NF-κB–mediated transcription (25), and they concluded that inhibition of 2 or more distinct targets will provide a foundation for the development of effective chemoprotective agents. However crucially, no molecular link was made between their observations using the different assays. Dufour and colleagues (43) and Yan and colleagues (44) have extended their work on the development of irreversible inhibitors of NQO1 (45). These agents deactivate NQO1 and NQO2 by alkylation of their active sites. However, this attractive mechanism-based approach also has limitations with regard to target selectivity (46). The work of Nolan and colleagues (3, 22, 23) and that reported here was undertaken with the specific objective of identifying novel inhibitors of NQO2 that might have therapeutic properties on the basis of the impact of NQO2 on NF-κB–mediated gene transcription that was previously suggested from genetic deletion studies (21, 30). Using a computational approach to mine the NCI Chemical data base, we discovered a remarkable variety of structural types that could potentially act as inhibitors of NQO2. The active site of NQO2 is a hydrophobic cavity, 17 Å in length and 7 Å wide, which can accommodate a range of polycyclic and polyaromatic ligands of different size and structure adopting a variety of binding modes and interactions. Among the inhibitors is NSC13000 and we have solved the structure of this compound cocrystalized with NQO2. This structure was used to aid in the construction of a structure–activity relationship between the computationally derived binding affinity of the compounds from the NCI and their experimentally measured inhibitory potency. A reasonable correlation was obtained that, considering the structural diversity of the compounds, provides confidence in the docking analysis and thus can provide leads for future drug development. This same miscellaneous set of compounds has the additional effect of modulating NF-κB activity. In addition, a recent study (47) showed that NSC13000 and NSC14229 could induce p53 function in renal carcinoma cells in a mechanism that did not involve genotoxic stress but was mediated by suppression of NF-κB. Furthermore, both compounds effectively suppressed both the basal and induced activity of NF-κB (47). If these cells contained significant levels of NQO2, then it is possible that the observed phenomenon may be mediated by this enzyme. Thus, there is good evidence to suggest a causual link between NQO2 inhibition and NF-κB function; however, whether this operates at the level of protein–protein interactions and/or maintaining local redox status (15) remains to be determined. There is no doubt that modulating NF-κB could have therapeutic antitumor activity (28, 29) and targeting NQO2 may be a useful method to achieve this. Finally, NQO2 inhibitors can have additional therapeutic effects, because it has been shown that the inhibitors, melatonin and imatinib, can protect against radiation-induced lung inflammation, a process thought to be due, in part, to TNF-dependent effects (48–50).

Disclosure of Potential Conflicts of Interest

No potential conflicts of interest were disclosed.

Acknowledgments

The authors thank the Drug Synthesis and Chemistry Branch, Developmental Therapeutics Program, Division of Cancer Treatment and Diagnosis, NCI for the supply of compounds and John Barnes, Soo Mei Chee, and Soraya Alnabulsi (University of Manchester) for the synthesis of NRH.

Grant Support

This work was supported by an grants from the MRC (G0500366) and AICR (08–0152).

The costs of publication of this article were defrayed in part by the payment of page charges. This article must therefore be hereby marked *advertisement* in accordance with 18 U.S.C. Section 1734 solely to indicate this fact.

Received July 27, 2011; revised October 10, 2011; accepted November 10, 2011; published OnlineFirst November 16, 2011.

References

1. Liao S, Williams-Ashman HG. Enzymatic oxidation of some non-phosphorylated derivatives of dihydronicotinamide. Biochem Biophys Res Commun 1961;10:208–13.
2. Foster CE, Bianchet MA, Talalay P, Zhao Q, Amzel LM. Crystal structure of human quinone reductase type 2, a metalloflavoprotein. Biochemistry 1999;38:9881–6.
3. Nolan KA, Caraher MC, Humphries MP, Bettley HA, Bryce RA, Stratford IJ. *In silico* identification and biochemical evaluation of novel inhibitors of NRH:quinone oxidoreductase 2 (NQO2). Bioorg Med Chem Lett 2010;20:7331–6.
4. Buryanovskyy L, Fu Y, Boyd M, Ma Y, Hsieh TC, Wu JM, et al. Crystal structure of quinone reductase 2 in complex with resveratrol. Biochemistry 2004;43:11417–26.
5. Jamieson D, Tung AT, Knox RJ, Boddy AV. Reduction of mitomycin C is catalysed by human recombinant NRH:quinone oxidoreductase 2 using reduced nicotinamide adenine dinucleotide as an electron donating co-factor. Br J Cancer 2006;95:1229–33.
6. Knox RJ, Jenkins TC, Hobbs SM, Chen S, Melton RG, Burke PJ. Bioactivation of 5-(aziridin-1-yl)-2,4-dinitrobenzamide (CB 1954) by human NAD(P)H quinone oxidoreductase 2: a novel co-substrate-mediated antitumor prodrug therapy. Cancer Res 2000;60:4179–86.
7. Ferry G, Hecht S, Berger S, Moulharat N, Coge F, Guillaumet G, et al. Old and new inhibitors of quinone reductase 2. Chem Biol Interact 2010;186:103–9.
8. Dinkova-Kostova AT, Talalay P. NAD(P)H:quinone acceptor oxidoreductase 1 (NQO1), a multifunctional antioxidant enzyme and exceptionally versatile cytoprotector. Arch Biochem Biophys 2010;501:116–23.
9. Celli CM, Tran N, Knox R, Jaiswal AK. NRH:quinone oxidoreductase 2 (NQO2) catalyzes metabolic activation of quinones and anti-tumor drugs. Biochem Pharmacol 2006;72:366–76.
10. Gaikwad NW, Yang L, Rogan EG, Cavalieri EL. Evidence for NQO2-mediated reduction of the carcinogenic estrogen ortho-quinones. Free Rad Biol Med 2009;46:253–62.
11. Iskander K, Paquet M, Brayton C, Jaiswal AK. Deficiency of NRH:quinone oxidoreductase 2 increases susceptibility to 7,12-dimethylbenz(a)anthracene and benzo(a)pyrene-induced skin carcinogenesis. Cancer Res 2004;64:5925–8.

12. Radjendirane V, Joseph P, Lee YH, Kimura S, Klein-Szanto AJ, Gonzalez FJ, et al. Disruption of the DT diaphorase (NQO1) gene in mice leads to increased menadione toxicity. J Biol Chem 1998;273:7382–9.
13. Long DJ 2nd, Iskander K, Gaikwad A, Arin M, Roop DR, Knox R, et al. Disruption of dihydronicotinamide riboside:quinone oxidoreductase 2 (NQO2) leads to myeloid hyperplasia of bone marrow and decreased sensitivity to menadione toxicity. J Biol Chem 2002;277:46131–9.
14. Tsvetkov P, Reuven N, Shaul Y. The nanny model for IDPs. Nat Chem Biol 2009;5:778–81.
15. Tolstonog GV, Deppert W. Metabolic sensing by p53: keeping the balance between life and death. Proc Natl Acad Sci USA 2010;107:13193–4.
16. Gong X, Kole L, Iskander K, Jaiswal AK. NRH:quinone oxidoreductase 2 and NAD(P)H:quinone oxidoreductase 1 protect tumor suppressor p53 against 20s proteasomal degradation leading to stabilization and activation of p53. Cancer Res 2007;67:5380–8.
17. Asher G, Tsvetkov P, Kahana C, Shaul Y. A mechanism of ubiquitin-independent proteasomal degradation of the tumor suppressors p53 and p73. Genes Dev 2005;19:316–21.
18. Asher G, Lotem J, Cohen B, Sachs L, Shaul Y. Regulation of p53 stability and p53-dependent apoptosis by NADH quinone oxidoreductase 1. Proc Natl Acad Sci USA 2001;98:1188–93.
19. Iskander K, Gaikwad A, Paquet M, Long DJ 2nd, Brayton C, Barrios R, et al. Lower induction of p53 and decreased apoptosis in NQO1-null mice lead to increased sensitivity to chemical-induced skin carcinogenesis. Cancer Res 2005;65:2054–58.
20. Ahn KS, Sethi G, Jain AK, Jaiswal AK, Aggarwal BB. Genetic deletion of NAD(P)H:quinone oxidoreductase 1 abrogates activation of nuclear factor-kappaB, IkappaBalpha kinase, c-Jun N-terminal kinase, Akt, p38, and p44/42 mitogen-activated protein kinases and potentiates apoptosis. J Biol Chem 2006;281:19798–808.
21. Ahn KS, Gong X, Sethi G, Chaturvedi MM, Jaiswal AK, Aggarwal BB. Deficiency of NRH:quinone oxidoreductase 2 differentially regulates TNF signaling in keratinocytes: up-regulation of apoptosis correlates with down-regulation of cell survival kinases. Cancer Res 2007;67:10004–11.
22. Nolan KA, Humphries MP, Barnes J, Doncaster Jr, Caraher MC, Tirelli N, et al. Triazoloacridin-6-ones as novel inhibitors of the quinone oxidoreductases NQO1 and NQO2. Bioorg Med Chem 2010;18:696–706.
23. Nolan KA, Humphries MP, Bryce RA, Stratford IJ. Imidazoacridin-6-ones as novel inhibitors of the quinone oxidoreductase NQO2. Bioorg Med Chem Lett 2010;20:2832–6.
24. Sun B, Hoshino J, Jermihov K, Marler L, Pezzuto JM, Mesecar AD, et al. Design, synthesis, and biological evaluation of resveratrol analogues as aromatase and quinone reductase 2 inhibitors for chemoprevention of cancer. Bioorg Med Chem 2010;18:5352–66.
25. Conda-Sheridan M, Marler L, Park EJ, Kondratyuk TP, Jermihov K, Mesecar AD, et al. Potential chemopreventive agents based on the structure of the lead compound 2-bromo-1-hydroxyphenazine, isolated from Streptomyces species, strain CNS284. J Med Chem 2010;53:8688–99.
26. Mailliet F, Ferry G, Vella F, Berger S, Cogé F, Chomarat P, et al. Characterization of the melatoninergic MT3 binding site on the NRH:quinone oxidoreductase 2 enzyme. Biochem Pharmacol 2005;71:74–88.
27. Rix U, Hantschel O, DŰrnberger G, Remsing RLL, Planyavsky M, Fernbach NV, et al. Chemical proteomic profiles of the BCR-ABL inhiibitors imatinib, nilotinib, and dasatinib reveal novel kinase and nonkinase targets. Blood 2007;110:4055–63.
28. Meylan E, Dooley AL, Feldser DM, Shen L, Turk E, Ouyang C, et al. Requirement for NF-κB signalling in a mouse model of lung adenocarcinoma. Nature 2009;264:104–10.
29. Huang S, Pettaway CA, Uehara H, Bucana CD, Fidler IJ. Blockade of NF-kappaB activity in human prostate cancer cells is assoicated with suppression of angiogenesis, invasion, and metastasis. Oncogene 2001;20:4188–97.
30. Hsieh TC. Antiproliferative effects of resveratrol and the mediating role of resveratrol targeting protein NQO2 in androgen receptor-positive, hormone-non-responsive CWR22Rv1 cells. Anticancer Res 2009;29:3011–7.
31. Winger JA, Hantschel O, Superti-Furga G, Kuriyan J. The structure of the leukemia drug imatinib bound to human quinone reductase 2 (NQO2). BMC Struct Biol 2009;9:7.
32. Kabsch W. Evaluation of single-crystal X-ray diffraction data from a position-sensitive detector. J Appl Cryst 1988;21:916–24.
33. Adams PD, Afonine PV, Bunkóczi G, Chen VB, Davis IW, Echols N, et al. PHENIX: a comprehensive Python-based system for macromolecular structure solution. Acta Crystallogr D Biol Crystallogr 2010;66:213–21.
34. Emsley P, Cowtan K. Coot: model-building tools for molecular graphics. Acta Crystallographica D Biol Crystalogr 2004;60:2126–32.
35. Mehibel M, Singh S, Chinje EC, Cowen RL, Stratford IJ. Effects of cytokine-induced macrophages on the response of tumor cells to Banoxantrone (AQ4N). Mol Can Ther 2009;8:1261–69.
36. Grafone T, Palmisano M, Nicci C, Martelli AM, Emanuela O, Storti S, et al. Monitoring of FLT3 phosphorylation status and its response to drugs by flow cytometry in AML blast cells. Hematol Oncol 2008;26:159–66.
37. Cavet ME, Harrington KL, Ward KW, Zhang JZ. Mapracorat, a novel selective glucocorticoid receptor agonist, inhibits hyperosmolar-induced cytokine release and MAPK pathways in human corneal epithelial cells. Molecular Vision 2010;16:1791–800.
38. Cheng Y, Prusoff WH. Relationship between the inhibition constant (K1) and the concentration of inhibitor which causes 50 percent inhibition (I50) of an enzymatic reaction. Biochem Pharmacol 1973;22:3099–108.
39. Nolan KA, Timson DJ, Stratford IJ, Bryce RA. *In silico* identification and biochemical characterization of novel inhibitors of NQO1. Biorg Med Chem Letts 2006;16:6246–54.
40. Nolan KA, Scott KA, Barnes J, Doncaster J, Whitehead RC, Stratford IJ. Pharmacological inhibitors of NAD(P)H quinone oxidoreductase, NQO1: structure/activity relationship and functional activity in tumour cells. Biochem Pharmacol 2010;80:977–81.
41. Scott KA, Barnes J, Whitehead RC, Stratford IJ, Nolan KA. Inhibitors of NQO1: Identification of compounds more potent than dicoumarol without associated off-target effects. Biochem Pharmacol 2011;81:355–63.
42. Poroikov VV, Filimonov DA, Ihlenfeldt WD, Gloriozova TA, Lagunin AA, Borodina YV, et al. PASS biological activity spectrum predictions in the enhanced open NCI database brower. J Chem Inf Comput Sci 2003;43:228–36.
43. Dufour M, Yan C, Siegel D, Colucci MA, Jenner M, Oldham NJ, et al. Mechanism-based inhibition of quinone reductase 2 (NQO2): selectivity for NQO2 over NQO1 and structural basis for flavoprotein inhibition. Chembiochem 2011;12:1203–8.
44. Yan C, Dofour M, Siegel D, Reigan P, Gomez JD, Shieh B, et al. Indolequinone inhibitors of NRH:Quinone Oxidoreductase 2 (NQO2). Characterization of mechanism of inhibition in both cell-free and cellular systems. Biochemistry 2011;50:6678–88.
45. Winski SL, Faig M, Bianchet MA, Siegel D, Swann E, Fung K, et al. Characterization of a mechanism-based inhibitor of NAD(P)H:quinone oxidoreductase 1 by biochemical, X-ray crystallographic, and mass spectrometric approaches. Biochemistry 2001;40:15135–42.
46. González-Aragón D, Alcaín FJ, Ariza J, Jódar L, Barbarroja N, López-Pedrera C, et al. ES936 stimulates DNA synthesis in HeLa cells independently on NAD(P)H:quinone oxidoreductase 1 inhibition, through a mechanism involving p38 MAPK. Chem Biol Interact 2010;186:174–83.
47. Gurova KV, Hill JE, Guo C, Prokvolit A, Burdelya LG, Samoylova E, et al. Small molecules that reactivate p53 in renal cell carcinoma reveal a NF-kappaB-dependent mechanism of p53 suppression in tumors. Proc Natl Acad Sci USA 2005;102:17448–53.
48. Serin M, Gülbaş H, Gürses I, Erkal HS, Yücel N. The histopathological evaluation of the effectiveness of melatonin as a protectant against acute lung injury induced by radiation therapy in a rat model. Int J Radiat Biol 2007;83:187–93.
49. Li M, Abdollahi A, Grőne HJ, Lipson KE, Belka C, Huber PE. Late treatment with imatinib mesylate ameliorates radiation-induced lung fibrosis in a mouse model. Radiat Oncol 2009;21:66.
50. Zhang M, Qian J, Xing X, Kong FM, Zhao L, Chen M, et al. Inhibition of the tumor necrosis factor-alpha pathway is radioprotective for the lung. Clin Cancer Res 2008;14:1868–76.